Journal of Molecular Liquids 307 (2020) 112997

Contents lists available at ScienceDirect

Journal of Molecular Liquids

journal homepage: www.elsevier.com/locate/molliq

Dichlorobiphenyls and chlorinated benzoic acids – Emergent soil pollutants in model bacterial membranes. Langmuir monolayer and Grazing Incidence X-ray Diffraction studies

Aneta Wójcik [a], Paulina Perczyk [a], Paweł Wydro [b], Marcin Broniatowski [a,*]

[a] Department of Environmental Chemistry, Faculty of Chemistry, Jagiellonian University in Kraków, Gronostajowa 2, 30-387 Kraków, Poland
[b] Department of Physical Chemistry and Electrochemistry, Faculty of Chemistry, Jagiellonian University in Kraków, Gronostajowa 2, 30-387 Kraków, Poland

ARTICLE INFO

Article history:
Received 2 February 2020
Received in revised form 23 March 2020
Accepted 25 March 2020
Available online 27 March 2020

ABSTRACT

The multi-decade worldwide application of polychlorinated biphenyls (PCB) leads to the problem of soil pollution. The production and application of PCB was banned, so the gradual decrease of their concentration in the soils was expected. On the contrary, novel sources of dichlorobiphenyls as PCB 11 were identified and these emergent pollutants are still emitted to the environment. Dichlorobiphenyls and some chlorobenzoic acids (CBA) are known as dead-end PCB metabolites – they accumulate in the soils and being toxic to microorganisms lead to the impoverishment of soil decomposer consortia. The toxicity of PCB and CBA is connected with their membrane activity and accumulation in the bacterial membranes. The correlation between the phospholipid composition of the bacterial membrane and the toxicity of PCB and CBA is unfortunately unknown limiting the effective selection of bacterial species for bioremediation of polluted soils. To shed light on these phenomena we applied binary phospholipid Langmuir monolayers as model bacterial membranes. With these models we studied the phenomena of dichlorobiphenyls and selected CBA molecules' incorporation and the effects exerted by these molecules on the ordering of the phospholipid molecules at the molecular scale. For the studies of the organization of the model membranes we applied Grazing Incidence X-ray Diffraction. It turned out that the model membranes rich in cardiolipin can accumulate more pollutant molecules than the models containing phosphatidylglycerols. The accumulation of the pollutants did not cause any significant changes in the 2D crystalline structure of the former models whereas the latter were profoundly modified.

1. Introduction

Polychlorinated biphenyls (PCB) were industrially applied fluids produced on large scale during >50 years between the thirties and seventies of the previous century [1–3]. Large amount of the estimated 1.3 Mt. of PCB produced globally was released to the environment; either to the atmosphere or to the soils [4,5]. PCB are toxic, persistent in the environment and recalcitrant in the soils, so their production in the USA was banned in the late seventies [6] and PCB were included in the first Annex A of the Stockholm Convention regarding persistent organic pollutants (POP) [7]. PCB were produced as complicated mixtures of congeners, for example Aroclors in the USA, differing in the number of chlorine substituents and the mode of their location around the biphenyl frame [8]. The final sink of PCB are the soils in which these chemicals can be slowly dechlorinated and degraded by some specified soil bacteria and filamentous fungi [9,10]. Thus; there was a notion around the environmental chemists that the concentration of PCB in the environment was gradually lowering and that the investigation of PCB and their influence on living organisms was quite old-fashioned. This attitude changed dramatically in 2008 when 3,3′-dichlorobiphenyl was discovered in the air samples collected in Chicago agglomeration and in other location at the Great Laurentian Lakes [11]. 3,3′-dichlorobiphenyl known under the abbreviation PCB 11 was not the component of Aroclors or other commercial PCB mixtures. Thus, it turned out obvious that there were different and present sources of PCB contamination. PCB 11 can be a volatilized product of bacterial degradation of other PCB, for example PCB 77 (3,3′,4,4′-tetrachlorobiphenyl) but it is also a by-product and degradation product of diarylidene azo-pigments produced annually on kilotone basis [12–15]. Thus, the presence of dichloro-PCB in the environment is also of crucial importance, as these volatile compounds can also adversely affect human and animal health [15–19]. Dichlorinated PCB were not included in the Stockholm Convention of POP, as they were considered not recalcitrant in the environment and less lipophilic, so less bioaccumulative, than other PCB congeners.

* Corresponding author.
E-mail address: broniato@chemia.uj.edu.pl (M. Broniatowski).

https://doi.org/10.1016/j.molliq.2020.112997

However, such an attitude is an oversimplification as dichlorinated PCB can be divided into two different classes: these having both chlorines substituted at one ring and these with the chlorines substituted to both rings. The former class is relatively easily transformed by bacteria to chlorinated benzoic acids (CBA), whereas the latter class is much more recalcitrant [20,21]. Finally, both classes can be degraded to differently substituted CBA. Both dichloro PCB and CBA are also considered dead-end products of PCB degradation in the soil [22]. These compounds not only accumulate in the PCB-polluted soils but exhibit toxicity toward multiple soil bacteria [23–25] and can limit plant germination and growth [26,27] and can be genotoxic to some species [28]. Therefore, the presence of dichloro-PCB and CBA in the soils usually leads to the impoverishment of the soil decomposer consortia as well as to significant decrease of the yields of crops. On the other hand, there are some bacterial species known which can strive on dichloro-PCB or CBA as a sole carbon source [20,29,30]. Such bacteria can be inoculated into the PCB-polluted soils for their bioremediation [31,32]. PCB and CBA because of their chlorination are membrane-active compounds and can affect the structure and function of the decomposer cellular membranes, which is probably one of the reasons of their toxicity [33,34]. However, the susceptibility of a bacterial membrane to environmental toxicants depends profoundly on its composition [35–37]. The composition of the membrane can be manipulated both by the proper selection of the bacterial species for bioremediation as well as by the application of the specific nutrients and fertilizers which also affect the membrane phospholipid composition [38]. By now the correlation between the bacterial membrane composition and its susceptibility to PCB or CBA incorporation is vastly unknown. To shed light on these environmentally important phenomena in the present studies we applied the multicomponent phospholipid Langmuir monolayers as model bacterial membranes to investigated their interactions with dichlorinated PCB and CBA. It should be underlined here that the behavior of PCB and CBA in the soil environment is much different. PCB are hydrophobic and in the soil remain adsorbed to the clay minerals or to the humus-like matter [39,40]. Such a polluted niche can be colonized by the bacteria, which would later have a stationary supply of PCB. On the other hand CBA are water soluble, so they are mobile in the soil environment and can suddenly appear changing the conditions in a niche colonized already by some decomposer consortium [41]. In our studies we tried to emulate both situations. Thus, the hydrophobic dichloro-PCB were already added to the phospholipid mixture at the stage of Langmuir monolayer formation; whereas the CBA were injected into the subphase below a particular monolayer condensed to the required degree of order. It was mentioned in multiple articles that the toxicity and recalcitrance of isomeric PCB or CBA depends on the substitution pattern [23,42]. Therefore in our studies we applied three different recalcitrant dichloro-PCB: 3,3′-dichlorobiphenyl which is the emerging environmental pollutant and its two isomers 2,2′-dichlorobiphenyl and 4,4′-dichlorobiphenyl. Regarding CBA we applied 2,5-dichlorobenzoic acid and 3,4-dichlorobenzoic acid. The former is the degradation product of PCB 52 and the latter of PCB 77 – two important components of the Arochlor mixtures [43]. Additionally we also investigated 2,4,6-tichlorobenzoic acid, which is a degradation product of more chlorinated PCB congeners. In our studies we investigated how the presence of dichlorobiphenyl, its substitution pattern and mole ratio affect the mechanical, microscopic and structural properties of the model bacterial membranes. On the other hand in the penetration experiments we studied how the sudden appearance of CBA in the subphase below the model membranes affects their physical properties and how it is connected with the membrane composition. In our studies we applied the Langmuir technique that is registered the surface pressure (π)-mean molecular area (A) isotherms and performed the penetration tests in which π vs time dependence after CBA injection was monitored. The texture of the monolayers during the experiments was visualized with the application of Brewster angle microscopy (BAM); whereas the structural changes were monitored with the application of Grazing Incidence X-ray (GIXD) technique.

2. Experimental

2.1. Chemicals

The phospholipids applied for the model membranes' preparation: 1,2-dimyristoyl-sn-glycero-3-phosphoethanolamine (DMPE), 1,2-dimyristoyl-sn-glycero-3-phospho-(1′rac-glycerol) (sodium salt) (DMPG) and 1′,3′-bis[1,2-dimyristoyl-sn-glycero-3-phospho]-glycerol (sodium salt), that is tetramyristoyl cardiolipin (TMCL) were purchased from Avanti Polar lipids as lyophilized powders of the purity >99%. These phospholipids were kept refrigerated at −20 °C to avoid any decomposition. The dichlorobiphenyls: 2,2′-dichlorobiphenyl (PCB 4), 3,3′-dichlorobiphenyl (PCB 11) and 4,4′-dichlorobiphenyl (PCB 15) as well as chlorinated benzoic acids: 2,5-dichlorobenzoic acid (2,5-CBA), 3,4-dichlorobenzoic acid (3,4-CBA) and 2,4,6-trichlorobenzoic acid (2,4,6-CBA) were bought from Sigma Aldrich as analytical standards of the purity >99%. The structural formulas of the investigated pollutants are shown in (Scheme 1). The solvents applied in the studies: spectroscopic grade chloroform (99,9%) stabilized by ethanol, HPLC grade methanol (99,9%) and HPCL grade ethanol (98%) were also purchased from Sigma-Aldrich. Milli-Q water of the resistivity of 18.2 MΩ·cm was produced in our laboratory with the application of Merck-Millipore Synergy water purification system.

2.2. Stock solutions

The phospholipid samples of ca 2–2.5 mg were weighted on Mettler-Toledo semi-micro trough (with the accuracy of 10 μg) and dissolved in 10 cm^3 volumetric flasks in the chloroform/methanol 9/1 v/v mixture. The concentration of these solutions was ca. 0.3 mM for DMPE and DMPG and ca. 0.15 mM for TMCL (due to its dimeric structure). The stock solutions were kept refrigerated at −20 °C. Regarding the isomeric dichlorobiphenyls ca. 1 mg of their samples were weighted and dissolved in chloroform/methanol 9/1 v/v mixture in 10 cm^3 volumetric flasks – corresponding to the concentrations of ca. 0.45 mM. 0.05 M stock solutions of the investigated CBAs for penetration experiments were prepared in ethanol. All the stock solutions were kept refrigerated at −20 °C.

2.3. Model membranes

Soil bacteria can be both Gram-negative and Gram-positive, which means that their membranes differ considerably. Gram-positive bacteria have a thick murein-rich cellular wall protecting one bilayer membrane [44,45]; whereas Gram negative bacteria do not have such a cellular wall, but their cells are surrounded by two double layer membranes – the outer rich in lipid A and the inner [46]. In our studies we intended to emulate the membrane of Gram positive bacteria and the inner membrane of Gram negatives. The dominating phospholipid class in the gram negative bacteria inner membranes is phosphatidylethanolamine (PE) which constitutes usually about 70% of the phospholipid molecules; whereas the anionic phospholipids: phosphatidylglycerols (PG) and cardiolipins (CL) constitutes the remaining 30% [47,48]. In contrast in the membranes of Gram-positive bacteria negatively charged phospholipids dominate constituting around 80% of all phospholipid molecules, while PE are in minority [49,50]. To emulate the phospholipid matrix of soil bacteria membranes we prepared four different model systems: two of them modeling the Gram-negative bacteria inner membranes and two of them the Gram-positive membranes. The composition of these models is summarized in Table 1.

The mixed binary phospholipid solutions were prepared from the stock solutions just before the experiments. The membranes doped with PCB were prepared by mixing the appropriate volumes of phospholipid and PCB stock solutions in glass vials just before the experiments.

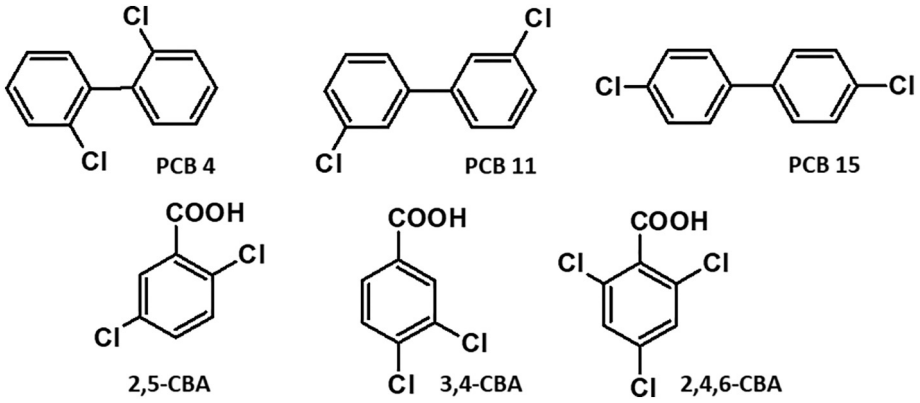

Scheme 1. Structural formulas of the investigated PCB and CBA

2.4. Techniques

2.4.1. Langmuir technique

Three different Langmuir troughs were applied during the experiments. The isotherms measurements and penetration tests were performed on a double barrier KN2002 Langmuir Blodgett trough (KSV-NIMA) of the nominal area of 275 cm^2 and the volume of 250 cm^3. In the BAM experiments a larger double barrier KSV-NIMA LB trough (KN 1006) of the area of 841 cm^2 was used. The GIXD experiments were performed on a custom-ordered Riegler&Kirstein (R&K) single barrier Langmuir trough of the area of approx. 500 cm^2. The management of the troughs was identical in all the experiments. After a finished experiment the monolayer material and the subphase were removed from the trough, which was later on washed with a tissue soaked in chloroform, followed by 2-propanol and rinsed with plentiful of MilliQ water. The troughs prepared to the experiment were filled by MilliQ water which we applied as the subphase. Appropriate volume of the pre-mixed chloroform solutions was drop-wise deposited at the air/water interface with the application of Hamilton analytical syringes. 10 min were left for chloroform evaporation after which the Langmuir monolayers were compressed with the compression rate of 20 $cm^2 \cdot min^{-1}$. All the experiments were performed at 20 °C with the application of Julabo water circulating bath for temperature control. Surface pressure was measured by w Wilhelmy-type electrobalance (NIMA-KSV) with a rectangular filtration paper plate (Whatmann) applied as surface pressure sensor. The accuracy of the measurement was 0.05 mN/m, whereas the uncertainty of the mean molecular area (A) was 1 $Å^2$/molecule. Each π-A isotherm was measured at least three times to guarantee the reproducibility of the experimental data. Compression modulus C_S^{-1} was calculated from the π-A isotherm data according to its definition: $C_S^{-1} = -A\frac{\partial \pi}{\partial A}$ [51].

2.4.2. Penetration tests

In penetration tests the model membranes were compressed to the required surface pressure value of 10, 20 or 30 mN/m, after which the compression was stopped and the monolayers were left for 20 min. to stabilize. After this time 500 μl of the 0.05 M ethanol solutions of 2,5-CBA, 3,4-CBA or 2,4,6-CBA were injected deep into the deposition well of the Langmuir trough via an injection port. The subphase in the deposition well was stirred by the magnetic stirrer to guarantee the uniform diffusion of the CBA molecules below the monolayers. In a set of blank experiments 500 μl of pure HPLC grade 98% ethanol were injected below the model membranes compressed to the above mentioned surface pressures. The injection of 500 μl of ethanol to the 250 cm^3 of the aqueous subphase had no measurable effect on the surface pressure value. After the injection of the CBA ethanol solutions the value of surface pressure was monitored during at least one hour and the results of the penetration tests were first presented in the form of the π-t curves.

Table 1
Composition of the applied model membranes expressed in mole proportions of the components.

Bacteria type	model	X(DMPE)	X(DMPG)	X(TMCL)
Gram negative	GNC	0.7	–	0.3
Gram negative	GNG	0.7	0.3	–
Gram positive	GPC	0.2	–	0.8
Gram positive	GPG	0.2	0.8	–

2.4.3. Brewster angle microscopy

UltraBAM instrument (Accurion GmbH, Goettingen, Germany) equipped with a 50 mW laser emitting p-polarized light at a wavelength of 658 nm, a 10× magnification objective, polarizer, analyzer and a CCD camera was used. The spatial resolution of the microscope was 2 μm. The foregoing apparatus and the Langmuir trough were placed on the table (Standa Ltd., Vilnius, Lithuania) equipped with active vibration isolation system (antivibration system VarioBasic 40, Halcyonics, Göttingen, Germany).

2.4.4. Grazing Incidence X-ray Diffraction (GIXD)

The experiments were performed on the SIRIUS beamline at SOLEIL synchrotron (Gif-sur- Yvette, France) using the dedicated liquid surface diffractometer. The detailed construction of the diffractometer working at the SIRIUS beamline and the parameters of the synchrotron beam applied in the GIXD experiments are described on the SOLEIL web site (www.synchrotron-soleil.fr) and in our previous papers [52,53] whereas the foundations of the technique are summarized in the excellent review articles [54,55].

3. Results and discussion

3.1. Interactions with dichlorobiphenyls

In the first step of our experiments we focused on the effects exerted on the model membranes by the isomeric dichlorobiphenyls: PCB 4, PCB 11 and PCB 15. The stock solutions were mixed to achieve the mole ratios of the investigated PCB of 0.1 and 0.3. It should be underlined that PCB are not amphiphilic; thus, do not exhibit surface activity and form neither adsorptive Gibbs nor deposited Langmuir monolayers. If added to a phospholipid mixture in a relatively low mole ratio and then deposited at the air/water interface they can build between the hydrophobic chains being an additional component of the model membrane or they can phase separate forming for example multilayer aggregates. In all the experiments the number of the phospholipid molecules deposited at the air/water interface was constant and to achieve the required mole ratios the total number of the molecules (phospholipid plus PCB)

was increased. In first experiments the π-A isotherms of the model membranes, that is sole phospholipid binary mixtures were measured. In the next step the isotherms at X(PCB) = 0.1 and X(PCB) = 0.3 were collected. As it was mentioned two options were possible: the incorporation of the PCB molecules into the monolayer or the formation of a separate phase. In the former situation the π-A isotherm should shift to larger mean molecular areas and possibly change its course as the number of film-forming molecules is higher. In the latter situation the isotherm should remain unchanged, that is the same as for the sole phospholipid monolayer as the PCB molecules are separated and do not interact with the components of the model membranes. The π-A isotherms and compression modulus – surface pressure (C_S^{-1}-π) dependences for the four model membranes – pure and doped with PCB are presented in Fig. 1.

There are some common features that can be observed for the four investigated model membranes regardless their composition. At X(PCB) = 0.1 in all the systems the isotherms are shifted toward the larger mean molecular area from the starting isotherm measured for the binary phospholipid mixtures. Thus, it can be inferred from that observation that all three investigated dichlorobiphenyls build into the model membranes. The second common feature is the overlapping of the isotherms at X(PCB) = 0.1 regardless the location of the chlorine atoms around the biphenyl frame. This fact can be explained assuming that at the low mole ratio of X(PCB) = 0.1 all the applied dichlorobiphenyl molecules were incorporated between the phospholipid molecules. The situation changes dramatically at X(PCB) = 0.3. First of all at this PCB mole ratio the investigated model membranes can be divided on two categories: these containing TMCL (GNC, GPC) and these containing DMPG (GNG, GPG). In the former systems much higher shifts of the isotherms toward greater mean molecular areas are observed than in the latter. Another trend can also be observed – the isotherms at X(PCB) = 0.3 shift to the larger mean molecular areas following the sequence: PCB 4 < PCB 11 < PCB 15. This trend is visible for all the investigated model membranes; however, in the systems with TMCL it is much pronounced. The incorporation of dichlorobiphenyls into the model membranes can be interpreted as the dissolution of these molecules in the microenvironment of the hydrophobic myristoyl chains. Thus, first of all it seems that it is easier to dissolve the PCB molecules in the monolayers containing TMCL than DMPG. It should be underlined that cardiolipins can be treated as bisphosphatidylglycerols; that is dimeric phospholipids containing four hydrocarbon chains [56]. Therefore, even if the mole ratio of the anionic phospholipids is the same – as for example 0.3 in the systems GNC and GNG the one with cardiolipin contains more myristoyl chains. Thus assuming that the PCB molecules are packed in the voids between the hydrophobic moieties of the phospholipid molecules it seems logical that more PCB molecules can be incorporated to the monolayers with TMCL than to these with DMPG. The system most rich in TMCL is GPC; thus, if the location of the chlorine atoms around the biphenyl frame is important for the packing of the PCB molecules between the hydrophobic chains, this system should much discriminate over the pollutants. As it is visible in Fig. 1 it really happens: PCB 4 shifts the isotherm ca. 10 Å^2/mol., PCB 11 ca. 15 Å^2/mol and PCB 15 > 20 Å^2/mol. PCB 4 is an example of the ortho,ortho-disubstituted PCB. PCB can be divided onto two classes: dioxin-like PCB in which no chlorine atom is substituted in the ortho, ortho' position and non-dioxin like PCB in which at least one chlorine atom is substituted therein. Only 12 congeners belong to the first class, whereas the remaining 197 congeners belong to the second [57]. The dioxin-like PCB are practically flat with both benzene rings located approximately in the same plane. If only one chlorine atom is present in the ortho position the planes of the benzene rings are twisted due to the steric interaction. It should be underlined that in PCB 4 both chlorine atoms are located in the ortho,ortho' position so the steric repulsion achieves its maximum leading to severe twist of

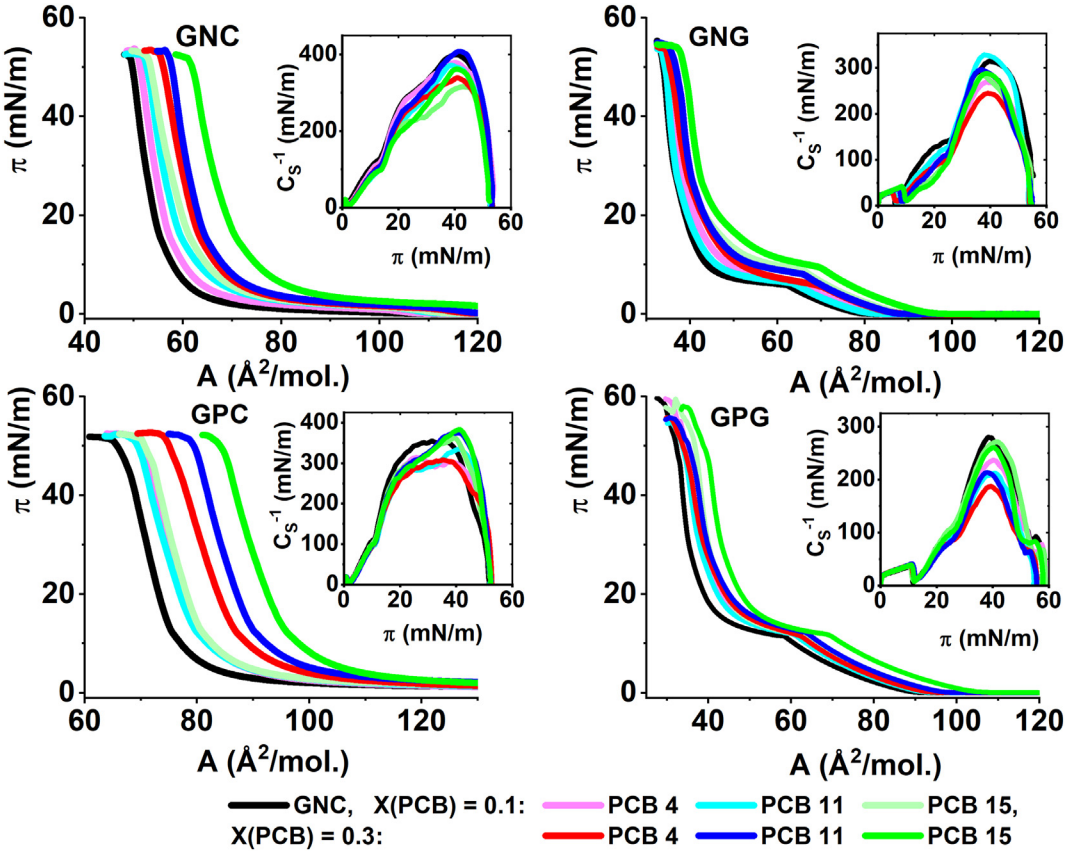

Fig. 1. π-A isotherms and ΔA-π plots (insets) for the investigated model bacterial membranes doped with dichlorobiphenyls.

the benzene ring planes. PCB 4 is the most bulky of the investigated here isomers, so its packing possibilities in the voids between the hydrocarbon chains are limited. The emerging environmental pollutant PCB 11 has its chlorine atoms located in the 3,3′ (metha,metha') positions. No ortho position is occupied so it can be assumed that the benzene rings can be nearly coplanar. Similar conclusion can be drawn for the 4,4′-dichloro isomer. However, in PCB 15 both chlorine atoms are located in the para,para' positions, that is lying on the main axis of the biphenyl moiety. PCB 15 is less bulky than PCB 11, which seems to be the reason of its best incorporation into the model membranes. It happens often that during the compression of a pollutant doped monolayer at a given surface pressure the pollutant is squeezed out of the phospholipid matrix. In such a situation starting from this surface pressure the π-A isotherm starts to overlap with the curve measured for an undoped model system. In the model membranes containing DMPG the isotherms really approach each other at higher surface pressure so it can be implied that at least a fraction of the PCB molecules is separated from the model membranes. On the contrary, nothing like this can be observed for GNC and GPC as at X(PCB) = 0.3 the ΔA values remain constant and >0 (between 10 and 20 Å^2/mol. depending on the PCB) even at high surface pressure value. Thus, the investigated dichlorobiphenyls seem to be permanently incorporated to the GNC and GPC model membranes and remain therein till the monolayer collapse.

To discuss the effects of PCB incorporation on the condensation of the model membranes we also calculated compression moduli upon the monolayers' compression (Fig. 1. insets). Differences between the C_S^{-1}-π curves for the model membranes and the membranes doped by PCB can be observed especially at higher surface pressures between 30 and 40 mN/m. In the systems with cardiolipin (GNC and GPC) these changes are not significant and not systematic, and taking under consideration the C_S^{-1} value the state of the monolayers can be described as solid [51]. More significant changes can be observed for the systems with DMPG, especially for the more bulky PCB 4. At X(PCB 4) = 0,3 for both GNG and GPG the maximal value of C_S^{-1} is lowered from 300 mN/m to ca. 200 mN/m, so it can be stated that according to the C_S^{-1} criterion the state of the monolayers was changed from solid to liquid condensed [51].

The evolution of the texture of the investigated monolayers was monitored upon their compression with the application of Brewster angle microscopy and the representative BAM photos are presented in Fig. 2.

At 10 mN/m dendritic condensed domains are present in the model membranes GNC, GNG, and GPC, whereas in the GPG monolayers first nuclei of such domains start to appear at 10 mN/m. The doping of the model membrane with dichlorobiphenyls considerably changes the monolayer textures. The introduction of PCB 4 leads to significant reduction of the domain diameters to ca. 10 μm from ca. 50 μm observed for the GNC model membrane. Similar trends can also be observed for the GNG and GPC models. In the case of the model membranes containing cardiolipin the introduction of PCB 4 leads to much closer packing of the smaller domains at the air/water interface. It should be underlined that the other two dichlorobiphenyls: PCB 11 and PCB 15 affect the domain morphology quite similarly – the domains are still dendritic, but their diameters are smaller than in the case of the pure model membranes. Thus, it is visible here that the structural difference between the ortho,ortho'-substituted PCB 4 and the other two dichlorobiphenyls, finds also its manifestation in the *meso* scale in the BAM images. Regarding the GPG model membrane the addition of PCB do not help the nucleation of the domains and the BAM images are homogeneous and dark proving the liquid expanded (LE) state of these monolayers. The images registered at π = 20 mN/m prove that the presence of PCB molecules profoundly affects the texture of the model membranes. The GPC model membranes doped with the PCBs are nearly homogeneous; whereas for the GNC and GNG model the fusion of the domains is also progressed. At 20 mN/m large liquid condensed domains (LC) of the diameter of ca. 50–70 μm are also present in the GPG model membrane; so at this pressure it is possible to observe the effects of PCB presence. Similarly to the previously discussed model systems also for GPG the doping with PCB lowers the diameter of the LC domains and changes their shape. Also here the textures of the monolayers doped by PCB 4 differ considerably from these doped with PCB 11 and PCB 15. The BAM microscopy was also applied for the observation of the monolayers at the higher X(PCB) of 0.3. The resultant photos taken at 10 and 20 mN/m are shown in the supporting materials. Qualitatively the images are very similar to these presented in Fig. 2, so the reorganization of the phospholipid chains takes place already at the appearance of PCB molecules in the model membrane and the further increase of their concentration does not lead to further evolution of the texture. The only difference between X(PCB) = 0.1 and 0.3 is the presence of multiple 3D aggregates visible in the photos taken at π = 20 mN/m and X (PCB) = 0.3 proving that at this PCB proportion some fraction of the molecules is eliminated from the monolayers upon their compression. The presence of the aggregates neither depends on the substitution mode of the chlorine atoms around the biphenyl frame nor the applied model of the bacterial membrane, so it can be inferred that the limit of PCB solubility within the model membranes lies somewhere between X(PCB) = 0.1 and X(PCB) = 0.3.

The model bacterial membranes were deliberately composed only of saturated phospholipids. It is of course a simplification of the real fatty acid chains distribution in which the cis-unsaturated and these containing cyclopropane ring are also widely populated [50,58]. On the other hand, such a selection of the phospholipids for our models enables the studies of the packing of the phospholipid molecules in the Ångstrom molecular scale with the application of the diffraction of synchrotron radiation. Indeed, PE, PG and CL with myristoyl chains form 2D crystalline monolayers as it was proved by multiple GIXD studies [59–61]. In our previous publication we proved that the applied here model bacterial membranes GNC, GNG, GPC and GPG are also 2D crystalline [62]. In the first three cases the packing of the myristoyl chains can be described by a hexagonal 2D crystalline lattice; whereas in the case of GPG the chains are collectively tilted from the monolayer normal which leads to the lowering of the lattice symmetry to centered rectangular. For consistence of the experimental results the GIXD data for the four model membranes were repeated and the results are presented in the Supporting Materials (SFig. 2 and SFig. 3).

In the present contribution we studied the effects of doping these model membranes with the investigated dichlorobiphenyls on their 2D crystallinity. For these studies we selected PCB 4 and PCB 15 as they profoundly differ in the chlorine substitution pattern. It turned out that the introduction of PCB 4 and PCB 15 to the closely packed GNC, GNG and GPC model membranes did not lead to noticeable changes in the diffraction data. The myristoyl chains were still hexagonally packed and there were no important differences in the lattice parameters or the ordering parameter L_{xy}. Therefore, the most interesting model membrane in this part of experiments was the GPG model, as only in this case significant differences were observed in the presence of dichlorobiphenyls. The GIXD results for these systems are presented in Fig. 3 whereas the calculated parameters are gathered in Table 2.

As it was already mentioned the packing of the myristoyl chains in the GPG model membrane is described by the centered rectangular 2D lattice with the chains tilted by the angle of 10.9° from the monolayer normal. The introduction of PCB 4 or PCB 15 into the monolayer leads to the condensing effect and in the presence of both molecules the myristoyl chains are oriented perpendicularly at the air/water interface. This results in the disappearance of the off-horizon signal in the I(Q_{xy}, Q_z) diffraction map. The only one diffraction signal with its intensity maximum located at $Q_z = 0$ visible in the B and C intensity maps proves the hexagonal packing of the scattering moieties. This result contradicts the conclusion drawn from the C_S^{-1}-π curves, that is the expansion effects observed for the GNG and GPG doped with PCB 4. However, it should be underlined that the compression modulus regards the whole monolayer treated as an elastic body; whereas the GIXD data

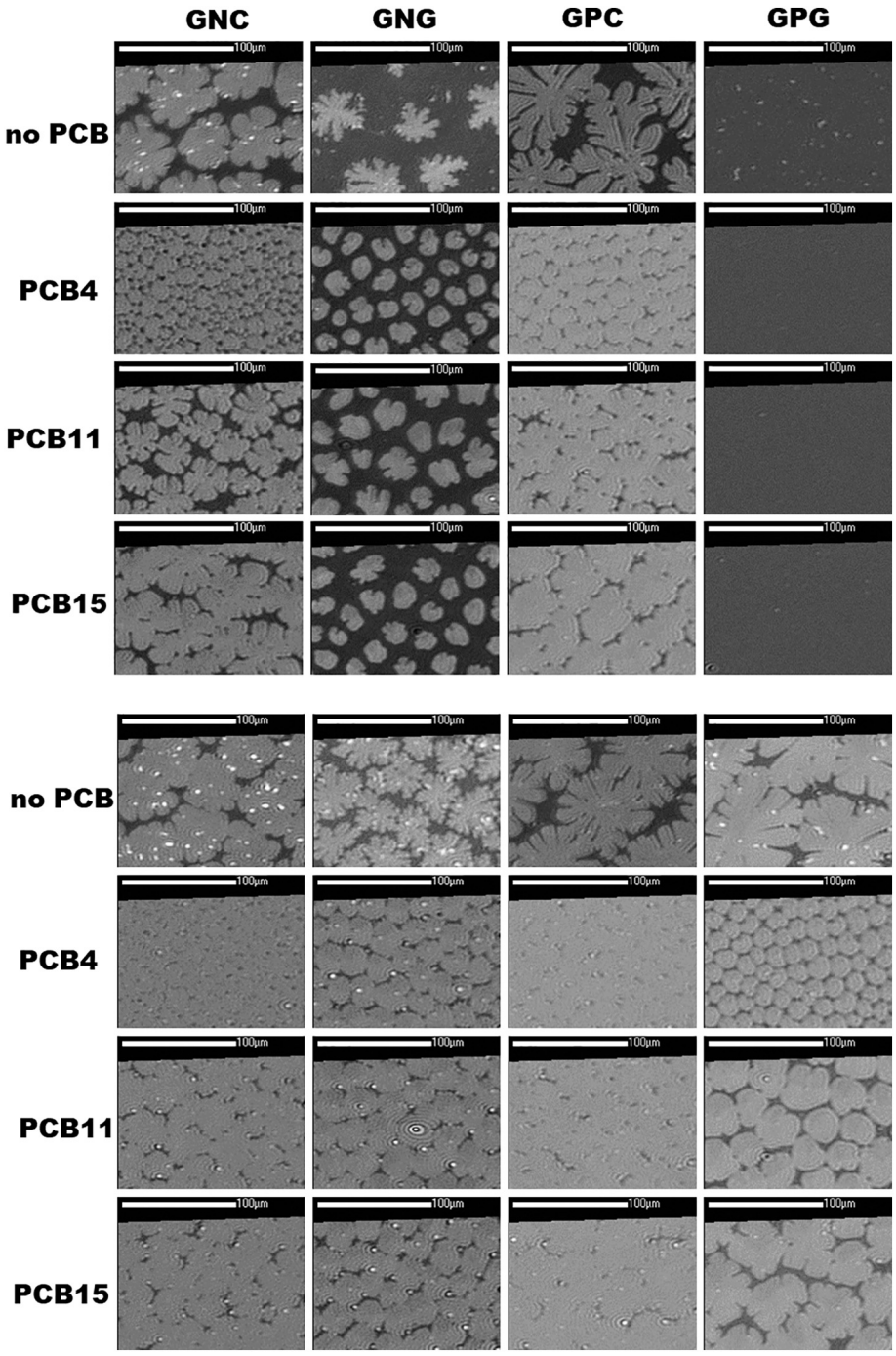

Fig. 2. Selected BAM images for the investigated systems at X(PCB) = 0.1. Upper panel – π = 10 mN/m, lower panel – π = 20 mN/m.

regard 2D crystalline nanodomains. Usually not all the monolayer is 2D crystalline and the crystalline domains are frequently in the equilibrium with amorphic entities [63]. In the global scale of the whole monolayer the presence of PCB 4 leads to the lowering of monolayer condensation. On the other hand in the nanoscale the presence of PCB 4 leads to the elimination of the tilt of the myristoyl chains, by which the mixed 2D crystalline domains achieve a more condensed arrangement.

3.2. The effects of the water soluble dichloro and trichlorobenzoic acids

In the subsequent part of our studies the effects of PCB metabolites, di and tri-chlorobenzoic acids were investigated. CBA are water soluble and can migrate in the soil solution and in the ground water within the aquifer. Therefore, the option of choice here were the penetration tests emulating the situation when the environmental niche (lacking of any chlorinated nutrients) is colonized by the decomposer consortium and suddenly the inflow of chlorinated substances occurs. The monolayers were compressed to the required surface pressure: 10, 20 or 30 mN/m, which enabled to achieve different degree of the phospholipid molecules ordering. Then the compression was stopped, the monolayer was relaxed at the required surface pressure value for 20 min after which the ethanol solution of the investigated CBA was injected deep into the well of the Langmuir trough. The evolution of surface pressure was monitored during at least one hour. At the beginning, just after the injection of the CBA solutions the experimental conditions were far from equilibrium, so usually a rapid increase of surface pressure was

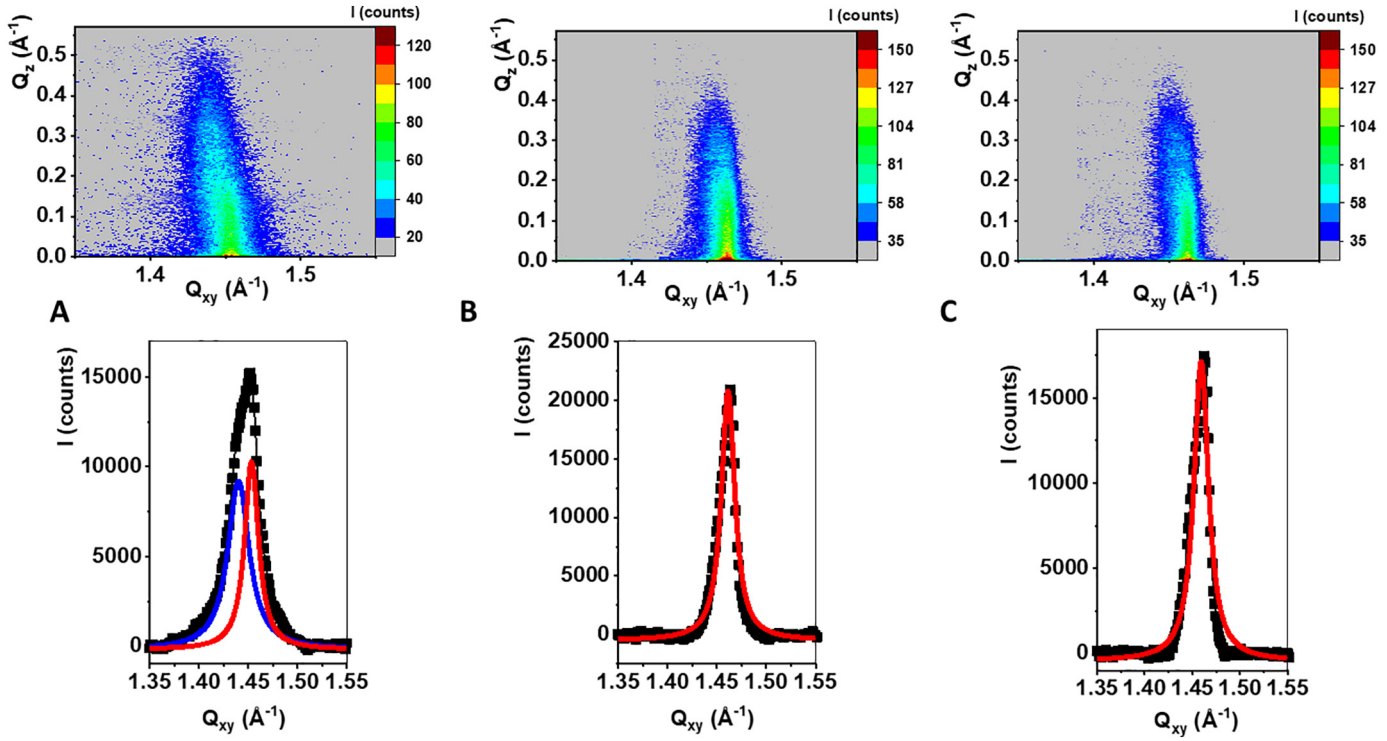

Fig. 3. GIXD data: Intensity maps $I(Q_{xy},Q_z)$ and Bragg peaks $I(Q_{xy})$ for the investigated systems: A) GPG, B) GPG doped by PCB 4 at X(PCB 4) = 0.3, C) GPG doped by PCB 15 at X(PCB 15) = 0.3. The experiments were performed at π = 25 mN/m.

observed in the first minutes after the injection. Then the systems gradually equilibrated approaching to the equilibrium surface pressure (π_{eq}) value. It can be inferred from the Δπ-t curves presented in Fig. 4 that the interactions of the CBAs with model membranes depend both on the monolayer composition as well as on the substitution pattern of the chlorine atoms. The second conclusion is especially interesting because it is in accordance with the biodegradation experiments' results proving exactly the same: for a given bacterial species its effectiveness in the degradation of isomeric CBA or vice versa the toxicity of the CBA toward the bacteria depends strongly on the substitution pattern of the chlorine atoms [23,42]. The resemblance between the in vitro biodegradation tests and Langmuir monolayer experiments proves that the model membrane approach is a valuable tool in the studies of the bacterial membrane – xenobiotic interaction. In our studies we tested two Gram negative and two Gram positive bacteria membrane models. For the Gram negative models: GNC and GNG compressed only to 10 mN/m 3,4-CBA turns out to incorporate most effectively as after the initial increase of 10 mN/m the surface pressure achieved finally the equilibrium value of 15 mN/m (Δπ = 5 mN/m) proving that the molecules of 3,4-CBA were incorporated permanently to the model membrane. The compression of the GNC and GNG monolayers modified the membrane environment changing the orientation and packing density of the myristoyl chains. This differentiated the GNC and GNG models considerably. GNC was susceptible to CBA incorporation whereas for GNG the Δπ values after equilibration were close to 0. For the GNC model 3,4-CBA and 2,4,6-CBA turned out to be more membrane active than 2,5-CBA as the equilibrium Δπ value of 5 mN/m proves the permanent built up of these metabolites to the membrane, whereas for 2,5-CBA Δπ was close to 0. At 30 mN/m the permanent incorporation of the investigated CBA molecules to the GNC and GNG model membranes was impossible. Regarding the models of the membranes of Gram positive bacteria, GPC and GPG, their behavior and the differences and similarities between them depended considerably on the experimental conditions. For the monolayers compressed to 10 mN/m the injection of the 3,4-CBA solution into the subphase perturbed considerably the organization of the GPC membrane, as initially the surface pressure rose to 25 mN/m (Δπ = 15); however, after equilibration Δπ stabilized at the level of 5 mN/m for both 3,4-CBA and 2,5-CBA, whereas the trisubstituted CBA was not effectively incorporated in these conditions. In subsequent experiments the model membranes were compressed to 20 mN/m. In these conditions for both GPC and GPG the injection of 3,4-CBA and 2,4,6-CBA caused significant and rapid increase of surface pressure (Δπ = 15 mN/m). After equilibration 3,4-CBA turned out to be most effectively detained in the membrane environment, as for this compound Δπ equilibrated at the level of 10 mN/m, whereas for the two other on the lower value of ca. 5 mN/m. Important differences between the GPC and GPG models were observed at 30 mN/m. It should be reminded that in these condition no incorporation of CBA was observed for the GN

Table 2
Structural parameters calculated from the GIXD data.

Sample	Q_{xy}, Q_z (Å^{-1}, Å^{-1})	a, b, γ (Å, Å, deg)	A (Å^2)	L_{xy} (Å)	τ (deg)
GPG	$Q_{xy<-1,1\geq}$ 1.440 $Q_{z<-1,1\geq}$ 0.24 $Q_{xy<0,2\geq}$ 1.453 $Q_{z<0,2\geq}$ 0	5.054, 8.649, 90	43.71 (A/2 = 21.88)	$L_{<-1,1\geq}$ 213 $L_{<0,2\geq}$ 325	10.9
GPG, X(PCB 4) = 0.3	Q_{xy} = 1.459 Q_z = 0	a = b = 4.973, 120	21.42	291	0
GPG, X(PCB 15) = 0.3	Q_{xy} = 1.461 Q_z = 0	a = b = 4.966, 120	21.35	325	0

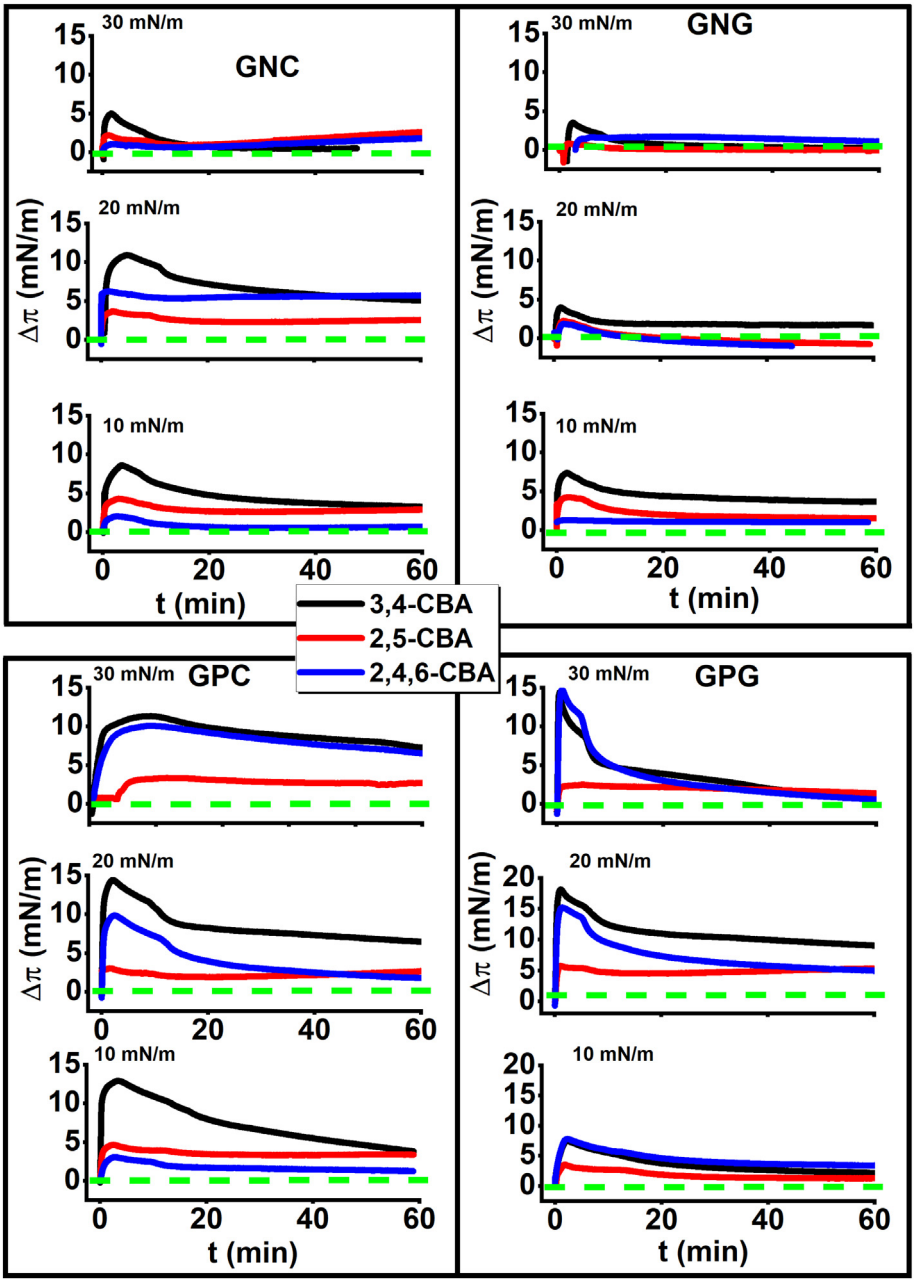

Fig. 4. Penetration experiments. The temporal (Δπ-t curves) evolution of surface pressure after the injection of 500 μl of 0.05 M ethanol solutions of the investigated CBAs to the subphase. The monolayers were stabilized at 10, 20 or 30 mN/m as indicated in the figure. Green dashed line denotes $\Delta\pi = 0$.

models. Here the injection of the 3,4-CBA and 2,4,6-CBA solutions induces a strong perturbation to the GP model membranes and the increase of surface pressure to 40–45 mN/m. Later on during the equilibration process profound differences between the GPC and GPG model membranes occurred. For 3,4-CBA and 2,4,6-CBA Δπ stabilized at the level of ca. 10 mN/m proving permanent incorporation of a considerable number of CBA molecules to the GPC model membrane, whereas for GPG Δπ stabilizes at ca. 2 mN/m for all three investigated CBA proving their limited built up into the membrane environment.

The above discussed penetration experiments proved that the interactions of CBA molecules with model bacterial membranes depend considerably on the substitution pattern of the chlorine atoms. The course of the Δπ-t curves and the values of equilibrium surface pressures indicate that in most of the investigated cases some CBA molecules remain permanently incorporated in the model membrane. Being located between the myristoyl chains the CBA molecules can also affect the packing of the phospholipid molecules in the molecular scale. To investigate these effects the GIXD method was applied. In the penetration tests 3,4-CBA turned out to be the most membrane active of all the investigated metabolites. Thus, in first turn the GIXD experiments were performed on 10^{-4} M 3,4-CBA solution. It turned out that for GPC and GNC model membranes the results were identical as on pure water; therefore they are not discussed here but presented in the supplementary materials (SFig. 4). In the systems GPG and GNG the presence of 3,4-CBA in the subphase lead to important structural changes; therefore these model membranes were also tested on the 10^{-4} M 2,5-CBA and 2,4,6-CBA solutions. The resultant GIXD data are presented in Fig. 5 for the GPG model membrane and in Fig. 6 for the GNG model. It should be underlined that the GIXD experiments were performed in different conditions than the penetration tests. During the GIXD experiments the Langmuir trough is closed in a helium flashed container and the injection of any solution into the subphase is impossible. Thus, the

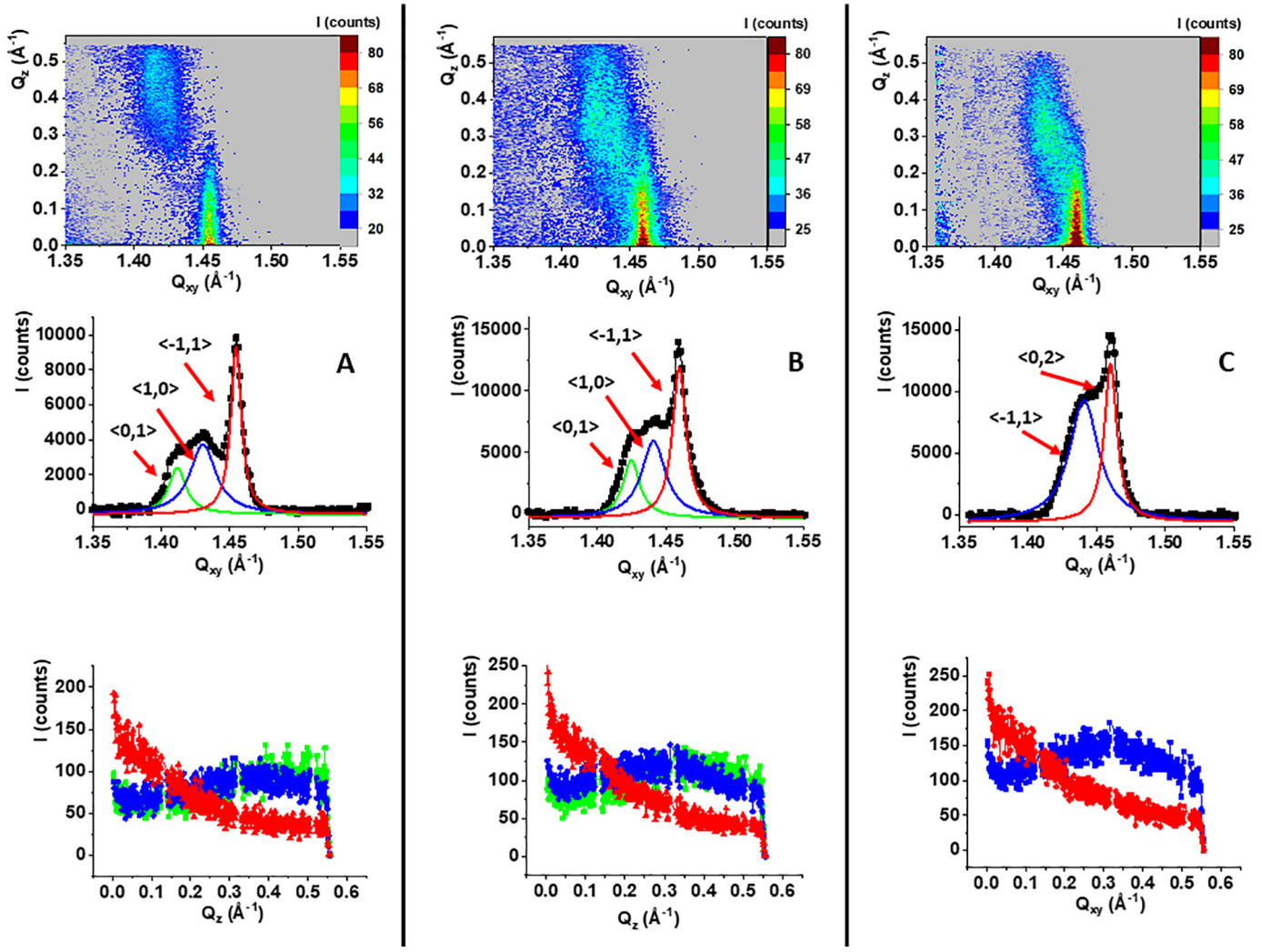

Fig. 5. GIXD data: $I(Q_{xy},Q_z)$ intensity maps, $I(Q_{xy})$ Bragg peak and $I(Q_z)$ Bragg rod profiles for the GPG model membranes spread on the 10^{-4} M solutions of: A) 3,4-CBA, B) 2,5-CBA, C) 2,4,6-CBA. The green, blue and red curves are Lorentz fits of the experimental data. The maxima are indexed with the Miller h.k indices. All the experiments were performed at 25 mN/m.

monolayers were spread already on a 10^{-4} M solutions of CBAs. Of course it can be supposed that it is easier for CBA molecules to build into the model membranes at low surface pressures at the beginning of their compression. However, as it was proved in the penetration tests after the initial sudden jump in the Δπ-t curves Δπ fell usually to much lower values and during the equilibration process multiple CBA molecules left the model membranes. In the GIXD experiments the monolayers were compressed to 25 mN/m and equilibrated for 20 min before the beginning of the diffraction experiment. Thus, it can be supposed that the conditions in the monolayers were comparable both in the penetration teste and the GIXD experiments regarding the presence of CBA in the monolayer.

The resultant GIXD data are presented in Fig. 5. Whereas the structural parameters extracted from the GIXD data are summarized in Table S1 in the supplementary materials.

The presence of both dichlorobenzoic acids in the subphase and its subsequent incorporation into the GPG membrane leads to the increase of the tilt of the myrisoyl chains from 10.9° observed on water via 17.4° on the 10^{-4} M 2,5-CBA to 18.6° on the 10^{-4} M 3,4-CBA solution. The increase of tilt angle is followed by the change of its azimuth from the next neighbor NN to the intermediate orientation. Consequently three diffraction signals can be seen in the intensity map – one with its intensity maximum very close to the horizon and two with their intensity maxima at higher Q_z values. Such a sequence of the diffraction signals is typical to the oblique 2D lattice [54,55]. Interestingly the observed effects are similar for both the isomeric dichlorobenzoic acids. This is in contrast to the penetration tests results which proved that 3,4-CBA is accumulated in the GPG model membrane more effectively than 2,5-CBA. The GIXD results prove that even if the number of the incorporated 2,5-CBA molecules is smaller than for 3,4-CBA they can still affect profoundly the packing of the myristoyl chains. On the contrary, the results obtained for the GPG model membrane spread on the 10^{-4} M 2,4,6-CBA solution are very similar to the results obtained on pure water. In both the cases two separate diffraction signals can be observed in the intensity map identifying the centered rectangular lattice. The presence of 2,4,6-CBA in the subphase leads to the increase of the tilt angle from 10.9° to 14.0° but the other structural parameters remain practically unchanged. This result is especially interesting. It was reported in scientific literature that the degradation products of PCB and chlorinated pesticides can be more toxic to soil bacteria than the mother compounds [22]. Moreover, some of them turn out to be the dead-end products which are not further degraded by the bacteria and accumulate in the soil. It is highly probable that the less chlorinated CBA fit better to the phospholipid hydrocarbon chains than the more bulky trichloro counterparts. Thus, the dichlorobenzoic acids migrate more effectively to the membrane and incorporated therein can lead to significant changes of the acyl chains ordering affecting the fluidity of the monolayer.

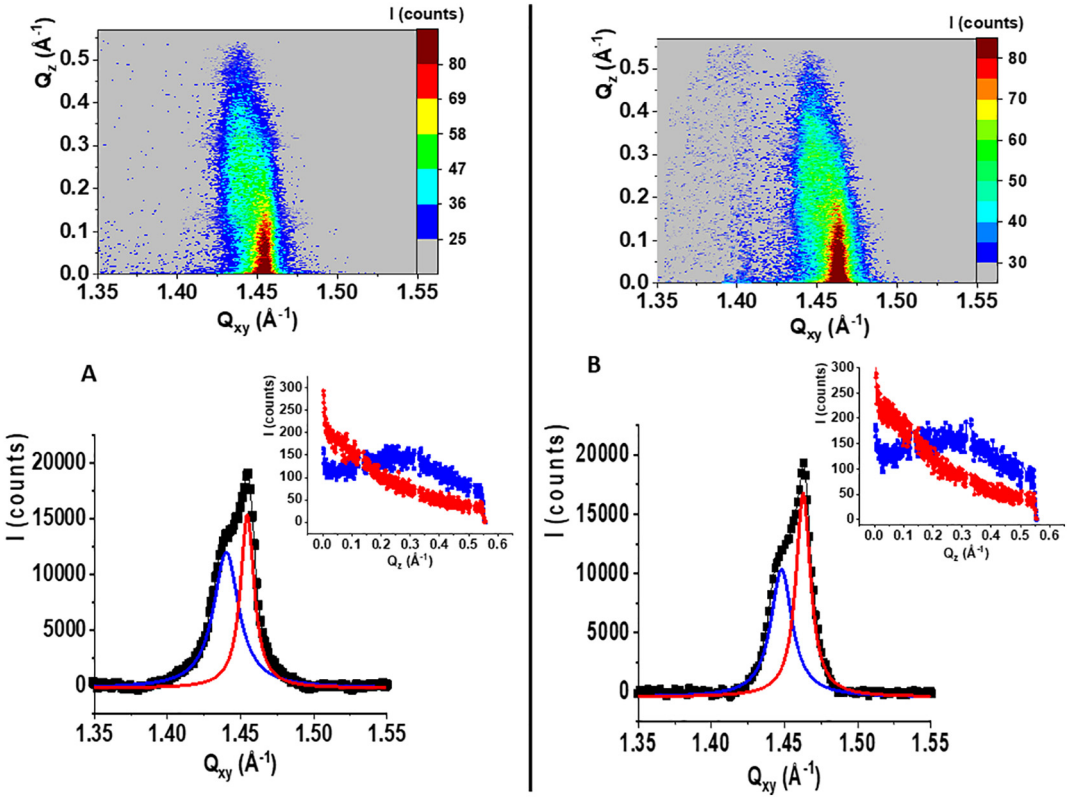

Fig. 6. GIXD results: $I(Q_{xy},Q_z)$ intensity maps, $I(Q_{xy})$ Bragg peak and $I(Q_z)$ Bragg rod profiles for the GNG model membranes spread on the 10^{-4} M solution of: A) 3,4-CBA; B) 2,5-CBA. The blue and red curves are Lorentz fits to the experimental data.

In both the cases there are two partially overlapped diffraction signals: one with its intensity maximum at $Q_z = 0$ Å^{-1} and the second with the intensity maximum at Q_z of ca. 0.25 Å^{-1}. This sequence of diffraction signals defines the rectangular centered 2D crystal lattice. The presence of the 3,4-CBA or 2,5-CBA in the subphase and their subsequent incorporation to the GNG model membrane induces the tilt of the myristoyl chains from the monolayer normal. Thus, it can be concluded that at the molecular level the model membranes containing DMPG are more easily rearranged by the presence of CBA than the cardiolipin-rich systems. On the other hand; the penetration tests proved significant accumulation of the CBA molecules also in the systems containing TMCL: GPC and GNC. TMCL has four hydrocarbon chains that pack tightly forming the hexagonal arrangement. In the presence of CBA this arrangement is preserved and the range of crystallinity (L_{xy}) is also similar on water and on the CBA solutions. Thus, it can be postulated that in the systems containing cardiolipin phase separation takes place at the nano scale and that some nanodomains form in the GPC and GNC model membranes, that is these containing cardiolipin. The nanodomains enriched in CBA are tightly packed but amorphous; whereas the phospholipid nanodomains are still 2D crystalline with hexagonally packed myristoyl chains. Such a phase separation in the nano scale cannot be postulated for the model membranes containing DMPG. In these systems CBA molecules are uniformly distributed between the myristoyl chains leading to the changes of their orientation at the air/water interface.

4. Conclusions

The interactions of emergent soil pollutants: dichlorobiphenyls and chlorinated benzoic acids with model bacterial membranes were investigated. Binary phospholipid Langmuir monolayers with their composition simulating Gram-negative and Gram-positive soil bacteria were applied. It turned out that the model membranes containing cardiolipin could host larger amounts of PCB or CBA pollutants than their counterparts containing phosphatidylglycerol. This observation was explained by the structural difference between CL and PG: cardiolipin is a dimeric phospholipid containing four hydrocarbon chains in its molecule. In the model membrane composed of phosphatidylethanolamine (PE) and CL or PG at the same mole ratio there is more hydrocarbon chains in the model containing CL than in this containing PG. Assuming that PCB or CBA are accumulated in the voids between the hydrocarbon chains there is more space for them in the CL-rich membrane. However, discussing biodegradation of persistent pollutants in the soils two factors should be considered. For their biodegradation the pollutants have to be transported to the membranes to enter the cell of the decomposer organism, so some accumulation of such hydrophobic nutrients in the membrane is unavoidable. On the other hand, the accumulated pollutants should not modify the structure of the membrane, especially regarding its fluidity. To assess the effects of PCB and CBA accumulation in the model membranes in the molecular scale the GIXD technique was applied. It turned out that the organization of the tightly packed CL-containing models: GPC and GNC were not affected neither by the presence of PCB nor by the presence of CBA molecules. On the contrary, the PG-containing models were susceptible to pollutant-caused rearrangements. The doping of the Gram positive bacteria membrane model GPG with dichlorobiphenyls (PCB 4 and PCB 15) lead to the change of the tilt angle of the myristoyl chains from 11^0 to 0. The 2D crystal lattice was changed from centered rectangular to hexagonal, which in the *meso* scale means the transition from the liquid condensed to the solid state of the monolayer. Thus, this experiment proves the possibility of membrane rigidification by the accumulated PCB molecules. On the contrary, the dichlorobenzoic acids: 3,4-CBA and 2,5-CBA caused the increase of molecular tilt and change of its azimuth when accumulated in the model membrane environment. The 2D lattice was changed from rectangular centered to oblique, which generally can be interpreted as the lowering of the myristoyl chains ordering. The experiments concerning both the PCB and CBA proved that the effectiveness of the pollutant incorporation in the membrane environment and the number of

accumulated molecules depend strongly on the substitution pattern of the chlorine atoms. Moreover, it was proved that dichlorinated CBA can exert a more disorganizing effect on the model membrane than their more chlorinated predecessors. This observation was in accordance with scientific literature as dichlorobenzoic acids are often dead-end products of PCB degradation in the soils, which is connected with their membrane activity and toxicity to decomposer organisms. From the perspective of the remediation of PCB-contaminated soils it can be inferred from our results that the bacteria, both Gram positive and negative, with large proportion of cardiolipin in their membranes could be effective in biodegradation processes. Such organisms could assimilate considerable amounts of chlorinated hydrophobic pollutants from their surrounding and accumulate them temporarily in their membranes without any negative effects for the membrane functioning.

CRediT authorship contribution statement

Aneta Wójcik: Investigation, Writing - original draft. **Paulina Perczyk:** Investigation, Writing - original draft. **Paweł Wydro:** Investigation, Methodology, Formal analysis. **Marcin Broniatowski:** Conceptualization, Funding acquisition, Supervision, Investigation, Validation, Writing - review and editing.

Declaration of competing interest

I would like herby to certify on myself and on behalf of my co-authors that there are no conflicts of interests regarding our contribution entitled “Dichlorobiphenyls and chlorinated benzoic acids – emergent pollutants in model bacterial membranes. Langmuir monolayer and grazing incidence X-ray diffraction studies”. The studies referred in our article were financed by the Polish National Science Centre (No 2016/21/B/ST5/00245).

Acknowledgements

This project was financed by the National Science Centre (No 2016/21/B/ST5/00245). We gratefully acknowledge SOLEIL for provision of synchrotron radiation facilities and we would like to thank Dr. Philippe Fontaine for assistance in using SIRIUS beamline.

Appendix A. Supplementary data

Selected BAM images for X(PCB) = 0.3. GIXD results for: the model membranes GNC, GNG, GPC and GPG spread on pure water and GNC and GPC spread on the 10^{-4} 3,4-CBA solution.Supplementary data to this article can be found online at doi: https://doi.org/10.1016/j.molliq.2020.112997.

References

[1] J. Borja, D.M. Taleon, J. Auresenia, S. Gallardo, Polychlorinated biphenyls and their biodegradation, Process Biochem. 40 (2005) 1999–2013.
[2] B. Hens, L. Hens, Persistent threats by persistent pollutants: chemical nature, concerns and future policy regarding PCBs—what are we heading for? Toxics 6 (2018) 1.
[3] A.V.B. Reddy, M. Moniruzzaman, T.M. Aminabhavi, Polychlorinated biphenyls (PCBs) in the environment: recent updates on sampling, pretreatment, cleanup technologies and their analysis, Chem. Eng. J. 358 (2019) 1186–1207.
[4] K. Breivik, A. Sweetman, J. Pacyna, K.C. Jones, Towards a global historical emission inventory for selected PCB congeners — a mass balance approach: 3. An update, Sci. Total Environ. 377 (2007) 296–307.
[5] P.D. Jepson, R.J. Law, Persistent organic pollutants, persistent threats. Polychlorinated biphenyls remain a major threat to marine apex predators such as orcas, Science 352 (2016) 1388–1389.
[6] L. Passatore, S. Rossetti, A.A. Juwarkar, A. Massacci, Phytoremediation and bioremediation of polychlorinated biphenyls (PCBs): state of knowledge and research perspectives, J. Hazard. Mater. 278 (2014) 189–202.
[7] chm.pops.int - Official Site of the Stockholm Convention, updated 2020.
[8] S.C. Chang, S.K. Lee, T.W. Chen, Effective removal of Aroclor 1254 and hexachlorobenzene in river sediments by coupling in situ phase-inversion emulsification with biological reductive dechlorination, J. Contamin. Hydrol. 221 (2019) 108–117.
[9] W.R. Abraham, B. Nogales, P.N. Golyshin, D.H. Pieper, K.N. Timmis, Polychlorinated biphenyl-degrading microbial communities in soils and sediments, Curr. Opin. Microbiol. 5 (2002) 246–253.
[10] T. Stella, S. Covinoa, E. Burianová, A. Filipová, Z. Křesinová, J. Voříšková, T. Větrovský, P. Baldrian, T. Cajthaml, Chemical and microbiological characterization of an aged PCB-contaminated soil, Sci. Total Environ. 533 (2015) 177–186.
[11] D. Hu, A. Martinez, K.C. Hornbuckle, Discovery of non-Aroclor PCB (3,3′-dichlorobiphenyl) in Chicago air, Environ. Sci. Technol. 42 (2008) 7873–7877.
[12] I. Basu, K.A. Arnold, M. Venier, R.A. Hites, Partial pressures of PCB 11 in air from several Great Lakes sites, Environ. Sci. Technol. 43 (2009) 6488–6492.
[13] R.A. Hites, Atmospheric concentrations of PCB 11 near the Great Lakes have not decreased since 2004, Environ. Sci. Technol. Lett. 5 (2018) 131–135.
[14] X. Hu, H.J. Lehmler, A. Adamcakova-Dodd, P.S. Thorne, Elimination of inhaled 3,3′-dichlorobiphenyl and the formation of the 4-hydroxylated metabolite, Environ. Sci. Technol. 47 (2013) 4743–4751.
[15] Y. Zhu, K.A. Mapuskar, R.F. Marek, W. Xu, H.J. Lehmler, L.W. Robertson, K.C. Hornbuckle, D.R. Spitz, N. Aykin-Burns, A new player in environmentally induced oxidative stress: polychlorinated biphenyl congener, 3,3′-dichlorobiphenyl (PCB 11), Toxicol. Sci. 136 (2013) 39–50.
[16] S. Alam, G.S. Carter, K.J. Krager, X. Li, H.J. Lehmler, N. Aykin-Burns, PCB 11 metabolite, 3,3′-dichlorobiphenyl-4-ol, exposure alters the expression of genes governing fatty acid metabolism in the absence of functional sirtuin 3: examining the contribution of MnSOD, Antioxidants 7 (2018) 121.
[17] D. Chung, R. Loch Caruso, Potential role for oxidative stress in 2,2′-dichlorobiphenyl–induced inhibition of uterine contractions but not myometrial gap junctions, Toxicol. Sci. 93 (2006) 172–179.
[18] S. Hou, M. Altarawneh, E.M. Kennedy, J.C. Mackie, R. Weber, B.Z. Dlugogorski, Formation of polychlorinated dibenzo- *p* -dioxins and dibenzofurans (PCDD/F) from oxidation of 4,4′-dichlorobiphenyl (4,4′-DCB), Proc. Combustion Inst. 37 (2019) 1075–1082.
[19] M.A. Roy, K.E. Sant, O.L. Venezia, A.B. Shipman, S.D. McCormick, P. Saktrakulkla, K.C. Hornbuckle, A.R. Timme-Laragy, The emerging contaminant 3,3′-dichlorobiphenyl (PCB 11) impedes Ahr activation and Cyp1a activity to modify embryotoxicity of Ahr ligands in the zebrafish embryo model (Danio rerio), Environ. Pollut. 254 (2019), 113027.
[20] S.A. Adebusoye, M.O. Ilori, F.W. Picardal, O.O. Amund, Metabolism of chlorinated biphenyls: use of 3,3′ and 3,5-dichlorobiphenyl as sole sources of carbon by natural species of Ralstonia and Pseudomonas, Chemosphere 70 (2008) 656–663.
[21] S.A. Adebusoye, F.W. Picardal, M.O. Ilori, O.O. Amund, C. Fuqua, N. Grindle, Growth on dichlorobiphenyls with chlorine substitution on each ring by bacteria isolated from contaminated African soils, Appl. Microbiol. Biotechnol. 74 (2007) 484–492.
[22] S.A. Adebusoye, M. Miletto, Characterization of multiple chlorobenzoic acid-degrading organisms from pristine and contaminated systems: mineralization of 2,4-dichlorobenzoic acid, Bioresour. Technol. 102 (2011) 3041–3048.
[23] G. Baggi, S. Bernasconi, M. Zangrossi, 3-Chloro-, 2,3- and 3,5-dichlorobenzoate co-metabolism in a 2-chlorobenzoate-degrading consortium: role of 3,5-dichlorobenzoate as antagonist of 2-chlorobenzoate degradation, Biodeg 16 (2005) 275–282.
[24] S.D. Siciliano, J.J. Germida, Degradation of chlorinated benzoic acid mixtures by plant-bacteria associations, Environ. Toxicol. Chem. 17 (1998) 728–733.
[25] P. Martínez, L. Agulló, M. Hernández, M. Seeger, Chlorobenzoate inhibits growth and induces stress proteins in the PCB-degrading bacterium *Burkholderia xenovorans* LB400, Arch. Microbiol. 188 (2007) 289–297.
[26] L.A. Brown, C. O'Leary-Steele, P. Brookes, L. Armitage, S. Kepinski, S.L. Warriner, A. Baker, Small molecule with differential effects on the PTS1 and PTS2 peroxisome matrix import pathways, Plant J. 65 (2011) 980–990.
[27] T. Nagaoka, J. Tanaka, K. Kouno, S. Yoshida, H. Tanaka, T. Ando, Generation of chlorinated aromatic acids during sludge-composting and their fate in soils, Soil Sci. Plant Nutr. 47 (2001) 443–453.
[28] T. Gichnera, P. Lovecka, B. Vrchotova, Genomic damage induced in tobacco plants by chlorobenzoic acids—Metabolic products of polychlorinated biphenyls, Mutation Res 657 (2008) 140–145.
[29] B.E. Jugder, H. Ertan, S. Bohl, M. Lee, C.P. Marquis, M. Manefield, Organohalide respiring bacteria and reductive dehalogenases: key tools in organohalide bioremediation, Frontiers Microbiol. 7 (2016)art 240.
[30] S. Kim, F. Picardal, Microbial growth on dichlorobiphenyls chlorinated on both rings as a sole carbon and energy source, Appl. Environ. Microbiol. 67 (2001) 1953–1955.
[31] R. Jing, S. Fusi, B.V. Kjellerup, Remediation of polychlorinated biphenyls (PCBs) in contaminated soils and sediment: state of knowledge and perspectives, Frontiers Environ. Sci. 6 (2018)art 79.
[32] T. Stella, S. Covino, M. Čvančarova, A. Filipova, M. Petruccioli, A. D'Annibale, T. Cajthaml, Bioremediation of long-term PCB-contaminated soil by white-rot fungi, J. Hazard. Mater. 324 (2017) 701–710.
[33] S. Zorádová, H. Dudášová, L. Lukáčová, K. Dercová, M. Čertík, The effect of polychlorinated biphenyls (PCBs) on the membrane lipids of Pseudomonas stutzeri, Int. Biodeterioration Biodegradation 65 (2011) 1019–1023.
[34] C. Totland, W. Nerdal, S. Steinkopf, Effects and location of coplanar and noncoplanar PCB in a lipid bilayer: a solid-state NMR study, Environ. Sci. Technol. 50 (2016) 8290–8295.
[35] F.P. Chavez, F. Gordillo, C.A. Jerez, Adaptive responses and cellular behavior of biphenyl-degrading bacteria toward polychlorinated biphenyls, Biotechnol. Adv. 24 (2006) 309–320.

[36] Claudia S. Lopez, A.F. Alice, H. Heras, E.A. Rivas, C. Sanchez-Rivas, Role of anionic phospholipids in the adaptation of Bacillus subtilis to high salinity, Microbiology 152 (2006) 605–616.
[37] C. Sohlenkamp, O. Geiger, Bacterial membrane lipids: diversity in structures and pathways, FEMS Microbiol. Rev. 40 (2016) 133–159.
[38] S. Zorádová-Murínová, H. Dudášová, L. Lukáčová, M. Čertík, K. Šilharová, B. Vrana, Adaptation mechanisms of bacteria during the degradation of polychlorinated biphenyls in the presence of natural and synthetic terpenes as potential degradation inducers, Appl. Microbiol. Biotechnol. 94 (2012) 1375–1385.
[39] M.R. Taha, S. Mobasser, Adsorption of DDT and PCB by nanomaterials from residual soil, PLoS One 10 (2015), e0144071.
[40] C. Flodin, E. Johansson, H. Boren, A. Grimvall, O. Dahlman, R. Morck, Chlorinated structures in high molecular weight organic matter isolated from fresh and decaying plant material and soil, Environ. Sci. Technol. 31 (1997) 2464–2468.
[41] L. Fava, M.A. Orrù, A. Crobe, A. Barra Caracciolo, E. Funari, Pesticide metabolites as contaminants of groundwater resources: assessment of the leaching potential of endosulfan sulfte, 2,6-dichlorobenzoic acid, 3,4-dichloroaniline, 2,4-dichlorophenol and 4-chloro-2-methylphenol, Microchem. J. 79 (2005) 207–211.
[42] S.A. Adebusoye, O.A. Adeosun, B.B. Olofinlade, Degradation of 2,5- and 3,4-dichlorobenzoic acids by bacterial species indigenous to rotten onion bulb and PCB-contaminated soil, Biocatal. Agricult. Biotechnol. 12 (2017) 248–252.
[43] B. Yilmaz, S. Sandal, C.H. Chen, D.O. Carpenter, Effects of PCB 52 and PCB 77 on cell viability, [Ca2+] levels and membrane fluidity in mouse thymocytes, Toxicol 217 (2006) 184–193.
[44] M. Rajagopal, S. Walker, Envelope structures of Gram-positive bacteria, Curr. Topics Microbiol. Immunol. 404 (2017) 1–44.
[45] N. Malanovic, K. Lohner, Gram-positive bacterial cell envelopes: the impact on the activity of antimicrobial peptides, Biochim. Biophys. Acta 1858 (2016) 936–946.
[46] T.J. Silhavy, D. Kahne, S. Walker, The bacterial cell envelope, Cold Spring Harb. Perspect. Biol. 2 (2010), a000414.
[47] S. Morein, A. Andersson, L. Rilfors, G. Lindblom, Wild-type Escherichia coli cells regulate the membrane lipid composition in a "window" between gel and non-lamellar structures, J. Biol. Chem. 271 (1996) 6801–6809.
[48] R.S. Conrad, H.E. Gilleland Jr., Lipid alterations in cell envelopes of polymyxin-resistant Pseudomonas aeruginosa isolates, J. Bacteriol. 148 (1981) 487–497.
[49] T.H.P. Nguyen, V.T.H. Pham, S.H. Nguyen, V. Baulin, R.J. Croft, B. Phillips, R.J. Crawford, E.P. Ivanova, The bioeffects resulting from prokaryotic cells and yeast being exposed to an 18 GHz electromagnetic field, PLoS One 11 (2016), e0158135.
[50] R.F. Epand, P.B. Savage, R.M. Epand, Bacterial lipid composition and the antimicrobial efficacy of cationic steroid compounds (Ceragenins), Biochim. Biophys. Acta 1768 (2007) 2500–2509.
[51] J.T. Davies, E.K. Rideal, Interfacial Phenomena, Academic Press, New York, 1961.
[52] M. Broniatowski, M. Flasiński, P. Wydro, Lupane-type pentacyclic triterpenes in Langmuir monolayers: a synchrotron radiation scattering study, Langmuir 28 (2012) 5201–5210.
[53] M. Broniatowski, M. Flasiński, P. Wydro, P. Fontaine, Grazing incidence diffraction studies of the interactions between ursane-type antimicrobial triterpenes and bacterial anionic phospholipids, Colloids Surf. B 128 (2015) 561–567.
[54] K. Kjaer, Some simple ideas on X-ray reflection and grazing-incidence diffraction from thin surfactant film, Physica B 98 (1994) 100–109.
[55] J. Als-Nielsen, D. Jacquemain, K. Kjaer, F. Leveiller, M. Lahav, L. Leiserowitz, Principles and applications of grazing incidence X-ray and neutron scattering from ordered molecular monolayers at the air-water interface, Physics Rep 246 (1994) 251–313.
[56] M. Schlame, M. Ren, The role of cardiolipin in the structural organization of mitochondrial membranes, Biochim. Biophys. Acta 1788 (2009) 2080–2083.
[57] A. Wójcik, A. Bieniasz, P. Wydro, M. Broniatowski, The effect of chlorination degree and substitution pattern on the interactions of polychlorinated biphenyls with model bacterial membranes, Biochim. Biophys. Acta 1861 (2019) 1057–1068.
[58] Y.Y. Chang, J.E. Cronan Jr., Membrane cyclopropane fatty acid content is a major factor in acid resistance of *Escherichia coli*, Molec. Microbiol. 33 (1999) 249–259.
[59] C.A. Helm, P. Tippmann-Krayer, H. Möhwald, J. Als-Nielsen, K. Kjaer, Phases of phosphatidylethanolamine monolayers studied by synchrotron X-ray scattering, Biophys. J. 60 (1991) 1457–1476.
[60] M. Broniatowski, M. Binczycka, A. Wójcik, M. Flasiński, P. Wydro, Polycyclic aromatic hydrocarbons in model bacterial membranes – Langmuir monolayer studies, Biochim. Biophys. Acta 1859 (2017) 2402–2414.
[61] F. Etienne, Y. Roche, P. Peretti, S. Bernard, Cardiolipin packing ability studied by grazing incidence X-ray diffraction, Chem. Phys. Lipids 152 (2008) 13–23.
[62] A. Wójcik, P. Perczyk, P. Wydro, M. Broniatowski, Incorporation of cyclodiene pesticides and their polar metabolites to model membranes of soil bacteria, J. Mol. Liq. 298 (2020), 112019.
[63] P.L.G. Chong, W. Zhu, B. Venegas, On the lateral structure of model membranes containing cholesterol, Biochim. Biophys. Acta 1788 (2009) 2–11.